

Ruthenium anchored on multi-walled carbon nanotubes: an efficient and reusable catalyst for the synthesis of xanthenes

Khalil Tabatabaeian¹ · Mohammad Ali Zanjanchi¹ ·
Manouchehr Mamaghani¹ · Ali Dadashi¹

Received: 7 July 2015 / Accepted: 30 October 2015
© Springer Science+Business Media Dordrecht 2015

Abstract A novel and highly efficient ruthenium-based catalyst was synthesized by immobilizing Ru(CO)₄ onto functionalized multi-walled carbon nanotubes. The catalyst was characterized by Fourier-transform infrared spectroscopy, X-ray diffraction, scanning electron microscopy, transmission electron microscopy, energy dispersive X-ray analysis, diffuse reflectance UV–Vis spectrophotometry, inductively coupled plasma and elemental analysis. This heterogeneous catalyst was successfully applied in the multi-component synthesis of various xanthene derivatives in good to excellent yields (28 samples, up to 96 % yield) under reflux condition and ultrasonic irradiation. The prepared catalyst was recovered four times without appreciable loss of activity.

Keywords Heterogeneous catalysis · Multi-walled carbon nanotubes · Ruthenium · Xanthenes · Ultrasound

Introduction

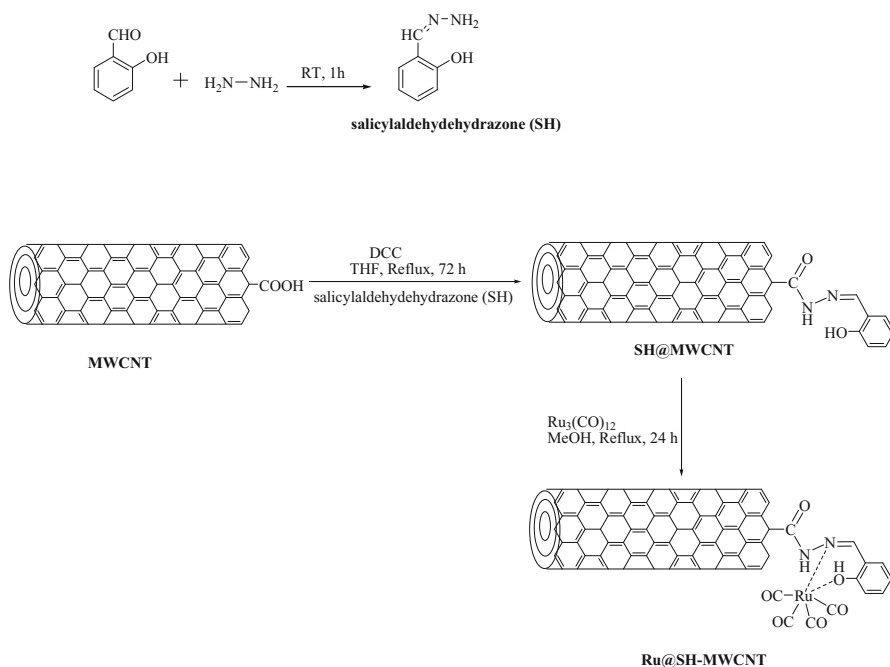
Multi-component reactions (MCRs) have emerged as a superior synthetic strategy in organic and medicinal chemistry. Productivity, selectivity, facile execution, synthetic convergence and atom economy are among the described merits of MCRs [1, 2]. Xanthenes, and especially benzoxanthenes, constitute an important class of organic compounds having wide range of therapeutic and biological properties, such as

Electronic supplementary material The online version of this article (doi:10.1007/s11164-015-2344-3) contains supplementary material, which is available to authorized users.

✉ Khalil Tabatabaeian
Taba@guilan.ac.ir

¹ Department of Chemistry, Faculty of Sciences, University of Guilan,
P. O. Box 41335-1914 Rasht, Iran

antibacterial, antiviral, antifungal, anti-depressant and anti-inflammatory activities [3, 4]. These heterocyclic compounds can be used as antagonists for paralyzing action of zoxazolamine [5], fluorescent material for visualization of biomolecules [6] and in laser technology [7]. Xanthene dyes are extracted from natural sources such as *Indigofera longiracemosa* [8]. Thus, the synthesis of xanthenes currently is of great importance. The conventional synthesis of 14-substituted-14-*H*-dibenzo[*a,j*]xanthenes involves the condensation of β -naphthol with aldehydes in the presence of different catalysts, such as sulfamic acid [9], I₂ [10], cyanuric chloride [11], HClO₄-SiO₂ [12], heteropolyacid [13], MeSO₃H [14], Dowex-50w [15], Yb(OTf)₃ [16], KAl(SO₄)₂·12H₂O (alum) [17], tetrabutylammonium bromide [18], proline triflate [19] P₂O₅/Al₂O₃ [20], RuCl₃·*n*H₂O [21], ZnO-NPs [22], sulfonic acid functionalized imidazolium salts (SAFIS) [23], polyvinylpyrrolidone-supported boron trifluoride [24], diatomite-SO₃H [25] and 1,3-disulfonic acid imidazolium hydrogen sulfate (DSIMHS) [26]. Synthetic 1,8-dioxo-octahydroxanthenes have been prepared through condensation reaction of aldehydes and 1,3-dicarbonyl compounds in the presence of various catalysts including, *p*-dodecylbenzenesulfonic acid [27], amberlyst-15 [28], trimethylsilylchloride [29], Fe³⁺-montmorillonite [30], (NH₄)₂-HPO₄ [31], SbCl₃/SiO₂ [32], silica sulfuric acid [33], ferric hydrogen sulfate [34] and [Et₃NSO₃H]Cl [35]. The straightforward approach for the synthesis of tetrahydrobenzo[*a*]xanthene-11-ones is the one-pot MCR between β -naphthol, aldehydes and dimedone by utilizing some catalysts such as strontium triflate [36], *p*-toluenesulfonic acid/ionic liquid ([bmim]BF₄) [37], indium trichloride [38], I₂ [39], tetrabutylammonium fluoride (TBAF) [40], HBF₄-SiO₂ [41], dodecatungstophosphoric acid [42], ceric ammonium nitrate (CAN) [43], RuCl₃·*n*H₂O [44] and succinimide-*N*-sulfonic acid [45]. However, despite the potential utility of aforementioned routes for the synthesis of xanthenes, some of them have their own disadvantages including low yields of products, long reaction times, drastic reaction conditions, tedious work-up procedures, or expensive reagents. Furthermore, in most of the reported methods, the catalysts are not recyclable. Sonochemistry is the best choice to overcome these limitations. A literature survey revealed that some methods have been reported for the synthesis of xanthenes under ultrasonic condition [46–52]. Ruthenium compounds are widely used as catalysts in organic synthesis [53, 54]. Although homogeneous ruthenium catalysts frequently exhibit very high activity, the difficulty of recovering the catalyst at the end of the process limits their application [55]. One of the possible approaches to overcome these drawbacks is their immobilization on solid supports [56–60]. The use of multi-walled carbon nanotubes (MWCNT) as new support materials is appealing due to the unique properties such as high surface area, chemical inertness, good mechanical strength and insolubility in most solvents. Moreover, their high surface allows higher loads of the catalytic sites in comparison with other supports such as Al₂O₃ or SiO₂ [61–66]. In continuation of our recent work [67], we have here explored an efficient strategy for the synthesis of a new ruthenium-bounded heterogeneous catalyst through functionalization of MWCNT with salicylaldehydehydrazone Schiff base ligand (SH), followed by complexation with Ru(CO)₄ (Ru@SH-MWCNT) (Scheme 1). This organic-inorganic hybrid material acts as an effective ruthenium catalyst for the synthesis of 14-aryl-14-*H*-



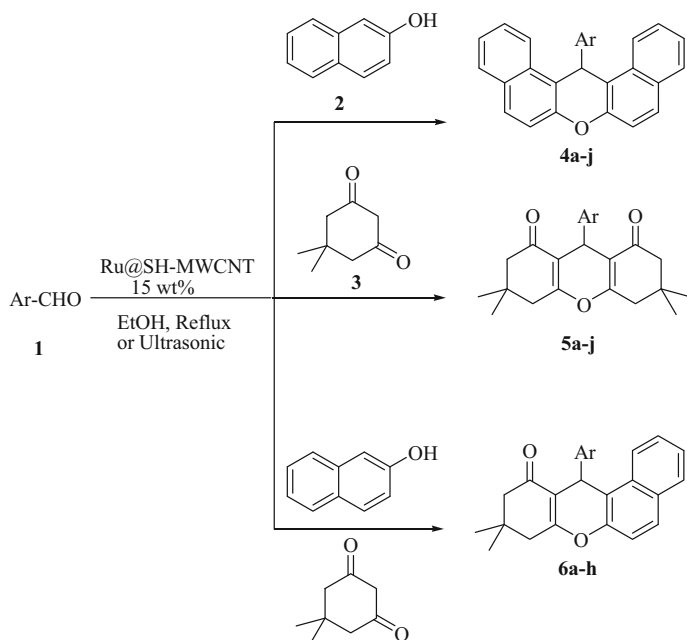
Scheme 1 Immobilization of ruthenium onto functionalized MWCNT

dibenzo[*a,j*]xanthenes (**4a–4j**), 1,8-dioxo-octahydroxanthenes (**5a–5j**) and tetrahydrobenzo[*a*]xanthene-11-ones (**6a–6h**) (Scheme 2).

Experimental

Materials and apparatus

All organic reagents and solvents were purchased from Merck and Fluka, and used as received. $\text{Ru}_3(\text{CO})_{12}$ (99 %) was purchased from Acros. MWCNTs containing $-\text{COOH}$ groups (MWCNT with inside diameters between 2 and 5 nm, outside diameters less than 8 nm, length between 10 and 30 μm , specific surface area more than $500 \text{ m}^2\text{g}^{-1}$, the COOH content, 3.8 wt% and purity $>95\%$) were purchased from Cheaptubes (USA). Powder XRD analysis was conducted on a Philips PW1840 diffractometer operated at 40 kV and 40 mA using $\text{Cu-K}\alpha$ radiation ($\lambda = 1.5418 \text{ \AA}$), over 2θ range $4^\circ\text{--}70^\circ$ at a scan rate of $0.1^\circ 2\theta/\text{s}$. The scan was performed at room temperature. SEM–EDX analyses were performed on a LEO 1430 VP instrument at accelerating voltage of 15 kV with an Au layer coating on carbon support. Transmission electron microscope (TEM) analysis was carried out using a Philips CM120 instrument operating at 120 kV. A small amount of powder sample was placed on the holey carbon grid of the transmission mode electron microscope. An ultrasound device Astra 3D (9.5 L, 45 kHz frequency, input power with heating, 305 W, number of transducers, 2) from TECNO-GAZ was used. The reactions were carried out in a round-bottomed flask of 25 mL capacity placed



Scheme 2 Synthesis of xanthenes catalyzed by Ru@SH-MWCNT

inside the ultrasonic bath containing water, 5 cm below the surface of the liquid. Diffuse reflectance spectra were recorded on a JASCOV-550 UV–Vis spectrophotometer at room temperature in the range of 230–800 nm using BaSO₄ as reference. The FT-IR spectra of the samples were recorded in transmission mode with a Bruker model Alpha spectrophotometer using KBr plates. The samples were ground with KBr and compressed into a pellet and placed into an IR cell. The spectra were recorded at room temperature after strip of the background in the region of 450–4000 cm⁻¹ with a resolution of 4 cm⁻¹ and the instrument acquiring 16 scans per sample. The ¹H NMR (500 or 400 MHz) and ¹³C NMR (125 or 100 MHz) were recorded at 298 K on a Bruker Avance spectrometer, by using TMS as internal standard and DMSO-d₆ or CDCl₃ as solvent. Signals are quoted in parts per million as δ downfield from tetramethylsilane (δ 0.00). Melting points were measured on a BUCHIB-540 melting point apparatus and are uncorrected. The metal loading was determined by inductively coupled plasma (ICP) (Labtam 8440 Plasma Laboratory) using a mixture of HNO₃/HCl (1/3 ratio) to dissolve the samples prior to the measurements. Elemental analysis was performed using a Carlo-Erba EA1110 CNNO-S instrument.

Catalyst preparation

Synthesis of salicylaldehydehydrazone: SH

Salicylaldehydehydrazone was prepared according to the reported method [68]. Salicylaldehyde (0.99 g, 8.2 mmol) dissolved in ethanol (5 mL) was added

dropwise to hydrazine hydrate (98 %) (2.06 g, 40.3 mmol) for 1 h at room temperature. After cooling in ice, the resulting shining white solid was filtered off, washed with diethyl ether and then dried under vacuum [Yield: 75.0 % (0.84 g), M.P.: 96–98 °C].

Grafting of salicylaldehydehydrazone onto MWCNT-COOH: SH@MWCNT

In a round-bottomed flask containing 20 mL of anhydrous THF and 1 g of MWCNT-COOH, salicylaldehydehydrazone (0.136 g, 1 mmol) and *N,N'*-dicyclohexylcarbodiimide (DCC) (0.206 g, 1 mmol) were added and the mixture was refluxed for 72 h. The mixture was centrifuged and the solid was washed with acetone and dichloromethane, respectively, and dried under vacuum overnight. The corresponding SH@MWCNT (1.03 g) was obtained. The loading of salicylaldehydehydrazone Schiff base ligand onto the MWCNT is 1.2 mmol/g, based on difference of the nitrogen content from MWCNT-COOH, as was revealed from CHN analysis.

Anchoring of Ru₃(CO)₁₂ onto SH@MWCNT: Ru@SH-MWCNT

A mixture of SH@MWCNT (1.0 g) and Ru₃(CO)₁₂ (0.160 g, 0.25 mmol) in methanol (20 mL) was stirred under reflux condition for 24 h. The solid phase was centrifuged and Soxhlet-extracted with ethanol and acetone and dried under vacuum overnight, leading to Ru@SH-MWCNT (1.04 g). The amount of ruthenium metal in the catalyst was found to be 5.60 wt% based on ICP analysis.

General procedure for the synthesis of 14-aryl-14-*H*-dibenzo[*a,j*]xanthenes

Method A

To a mixture of β-naphthol (2 mmol) and aldehyde (1 mmol) in ethanol (5 mL), Ru@SH-MWCNT (15 wt% based on all substrates) was added and the mixture was heated at 100 °C in an oil bath and stirred magnetically. After completion of the reaction, as indicated on thin-layer chromatography (TLC), the solvent was evaporated and chloroform was added to the mixture and centrifuged to separate the catalyst. Then, the solvent of the filtrate was evaporated and the residue was purified by recrystallization from ethanol. The isolated catalyst was washed thoroughly with ethyl acetate and acetone, dried under vacuum overnight and reused for further reaction cycles. All the products were identified by comparison of their physical and spectral data with those reported in the literature.

Method B

A mixture of β-naphthol (2 mmol), aldehyde (1 mmol) and Ru@SH-MWCNT (15 wt% based on all substrates) was charged into a round-bottomed flask, to which 5 mL of ethanol was added. Then, the reaction mixture was subjected to ultrasonic irradiation at 40 °C. After completion of the reaction (as was monitored by TLC),

the same workup as method A gave pure product and the catalyst was recovered and reused for successive reactions.

Typical procedure for the preparation of 1,8-dioxo-octahydroxanthenes

Method A

In a round-bottomed flask equipped with a magnetic bar and condenser, dimedone (2 mmol), aldehyde (1 mmol) and Ru@SH-MWCNT (15 wt% based on all substrates) were added to ethanol (5 mL). Then, the reaction mixture was refluxed at 80 °C for the appropriate time. Upon completion of the reaction (TLC monitoring), the solvent was evaporated. Chloroform was added and the mixture was centrifuged to separate the catalyst. Then, the filtrate was evaporated to dryness under reduced pressure to get the crude product which was directly recrystallized from ethanol.

Method B

In another procedure, the components as mentioned above were mixed thoroughly and sonicated at 40 °C for appropriate time. After completion of the reaction, as indicated by TLC, the reaction was worked up as described in method A.

General procedure for the synthesis of tetrahydrobenzo[*a*]xanthene-11-one derivatives

Method A

A mixture of aldehyde (1 mmol), β -naphthol (1 mmol) and dimedone (1.2 mmol) was added to a round-bottomed flask containing Ru@SH-MWCNT (15 wt% based on all substrates) and ethanol (5 mL), and the resulting mixture was refluxed at 80 °C for the appropriate time. After completion of the reaction confirmed by TLC, the solvent was evaporated. Chloroform was added and the mixture was centrifuged to separate the catalyst. Then, the solvent of the filtrate was evaporated and the resulting solid was purified by recrystallization from ethanol to afford the desired product.

Method B

A mixture of aldehyde (1 mmol), β -naphthol (1 mmol), dimedone (1.2 mmol) and Ru@SH-MWCNT (15 wt% based on all substrates) in 5 ml of ethanol was exposed to ultrasonic irradiation at 40 °C for the appropriate time. At the end of reaction, monitored by TLC, the work-up and purification of the products were performed as mentioned in method A.

Results and discussion

Catalyst characterization

The FT-IR spectroscopy was used to characterize the covalent grafting reactions (Fig. 1). The FT-IR spectra of MWCNT, SH@MWCNT and Ru@SH-MWCNT are shown in Fig. 1. All of them exhibited common bands at around 1200, 1570 and 3730 cm^{-1} corresponding to the stretching vibrations of C–C–C, C=C and –OH groups of the carbon nanotubes framework, respectively [69, 70]. In the spectrum of MWCNT-COOH, the expected vibration band of –C=O groups appeared at 1730 cm^{-1} (Fig. 1a). The FT-IR spectrum of SH@MWCNT is shown in Fig. 1b. The observed peak at 1699 cm^{-1} can be assigned to the stretching vibration of acidic and amidic carbonyl groups, which overlap. The peak of the azomethine group was masked with a broad band at 1552 cm^{-1} and cannot be resolved. The

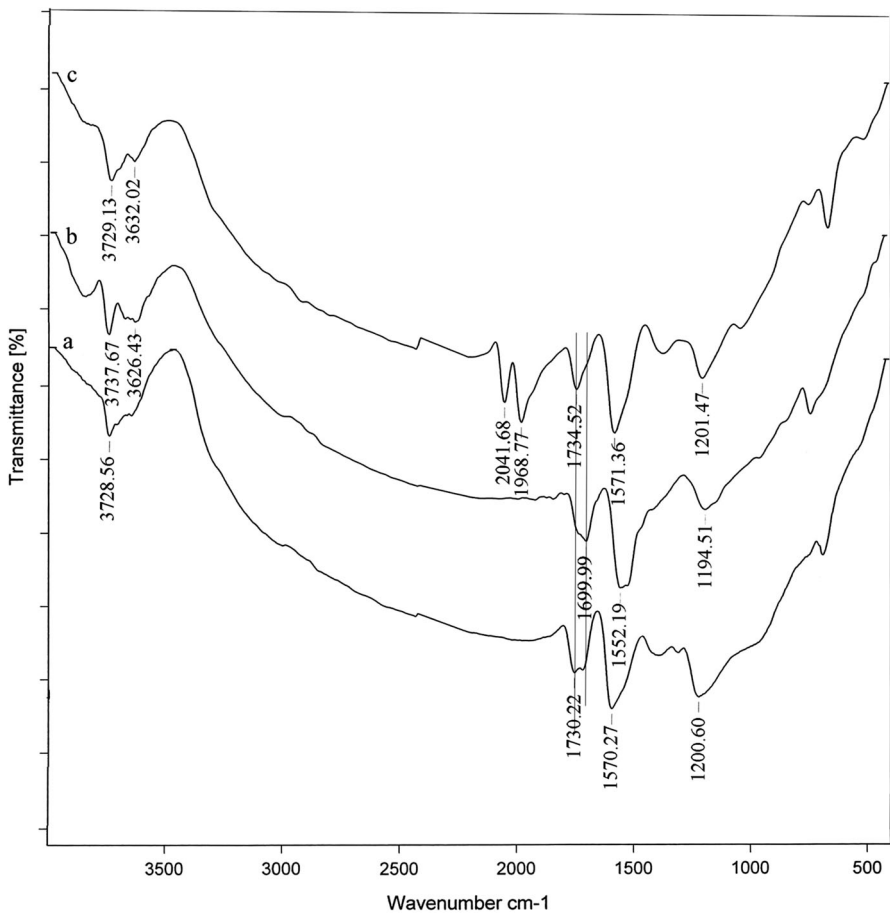


Fig. 1 IR spectra of **a** MWCNT, **b** SH@MWCNT and **c** Ru@SH-MWCNT

band at 3626 cm^{-1} was assigned to the stretching vibration of the N–H group (Fig. 1b). The spectrum of Ru@SH-MWCNT is shown in Fig. 1c. Thermal decomposition of the ruthenium cluster and elimination of two carbon monoxide groups from the coordination sphere of ruthenium afforded the precursor complex $\text{Ru}(\text{CO})_4$ [67]. After coordination with salicylaldehydrazone Schiff base ligand, a six-coordinated stable complex was formed. Complexation of ruthenium was confirmed by the appearance of two new bands at 1968 and 2041 cm^{-1} corresponding to the carbonyl ligands which is different from the stretching frequency of the CO groups of $\text{Ru}_3(\text{CO})_{12}$ at $2000\text{--}2050\text{ cm}^{-1}$. After immobilization of the ruthenium complex, electron pairs of nitrogen are involved in coordination and the resonance between the carbonyl group and nitrogen is prevented; thus, the stretching vibration of amidic carbonyl group is shifted to the upper frequency at 1734 cm^{-1} (Fig. 1c). The FT-IR data of the materials are listed in Table 1. In order to have covalent attachment of ruthenium onto the surface of MWCNT, two possible states can be considered in which the formation of a stable hexagonal chelate ring is most probable (Scheme 3).

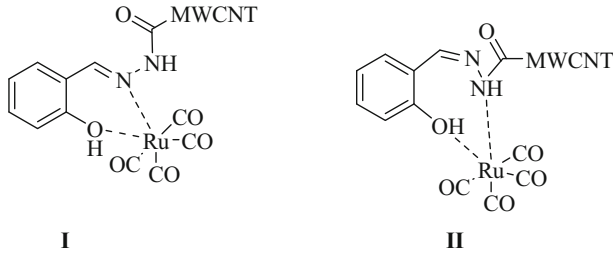
The structural features of MWCNT before and after functionalization were checked by X-ray diffraction studies (Fig. 2). The peaks at 2θ values of 26° and 43° were attributed to the (002) and (100) planes of the graphite structure of MWCNT. These were observed in all the XRD patterns and clearly indicate that the ordered structure of the materials was not altered during the functionalization treatment [69, 70]. However, upon the treatment for the anchorage of ruthenium to SH@MWCNT, little destruction of the structure occurred. Moreover, the diffraction lines were broadened and this shows that the particles are in the nanometer scale. The small shift of the main reflection toward lower angles for the SH@MWCNT in comparison with MWCNT could be due to the functionalization treatment or the anchoring of Schiff base complex which is loaded inside the MWCNT channels.

The surface morphology of the parent MWCNT and the prepared catalyst were examined by using a scanning electron microscope, and the corresponding images are presented in Fig. 3. Following the immobilization of ruthenium, the MWCNTs appear thicker due to the homogenous coating of the complex onto the surface of the carbon nanotubes [71]. Both samples showed that the nanotubes are aggregated.

The TEM image of the prepared catalyst showed that the tubular nature of MWCNTs was retained during the synthetic procedures (Fig. 4). No distinct XRD diffraction peak for ruthenium can be detected, implying that the metal has been homogeneously dispersed over the MWCNT surfaces.

Table 1 FT-IR data of materials

Material	$\nu_{\text{C-C}}$ (cm^{-1})	$\nu_{\text{C=C}}$ (cm^{-1})	$\nu_{\text{C=O}}$ (cm^{-1})	ν_{CO} (cm^{-1})	$\nu_{\text{N-H}}$ (cm^{-1})	$\nu_{\text{O-H}}$ (cm^{-1})
MWCNT-COOH	1200	1570	1730	–	–	3728
SH@MWCNT	1194	1552	1699	–	3626	3737
Ru@SH-MWCNT	1201	1571	1734	1968, 2041	3632	3729



Scheme 3 Two possible states for the coordination of Schiff base ligand to ruthenium

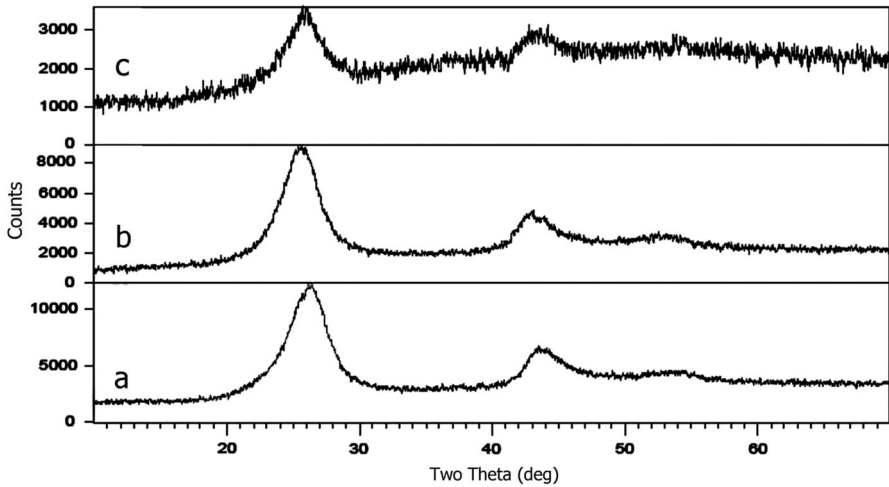


Fig. 2 X-ray diffraction patterns of **a** MWCNT, **b** SH@MWCNT, **c** Ru@SH-MWCNT

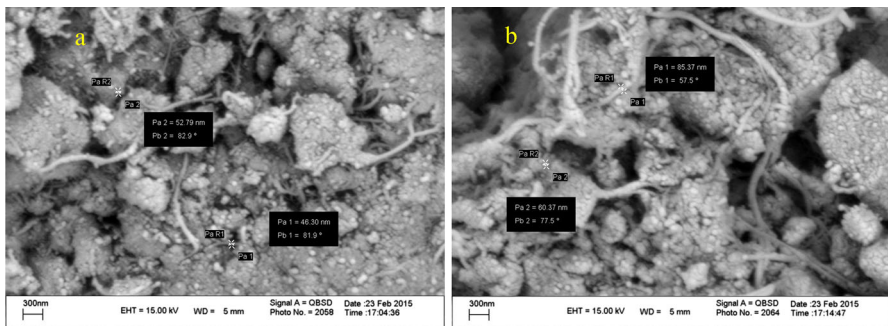


Fig. 3 SEM images of **a** MWCNT, **b** Ru@SH-MWCNT

In the EDX spectra of catalyst, the small peaks for ruthenium in the region of 2.5–2.8 keV clearly indicate the presence of ruthenium on the surface of the MWCNT (Fig. 5).

Further evidence for the incorporation of ruthenium onto the MWCNT was provided by UV–Vis spectroscopy in the diffuse reflectance mode. Salicylaldehyde-hydrazone Schiff base ligand (SH) has a strong absorption peak at 356 nm and a shoulder at 382 nm assigned to $n \rightarrow \pi^*$ and $\pi \rightarrow \pi^*$ transitions in the aromatic moiety and azomethine group [68]. In the spectrum of MWCNT, there are two absorption bands at 368 and 467 nm corresponding to $n \rightarrow \pi^*$ and $\pi \rightarrow \pi^*$ transitions of the C=C and C=O bonds. The ruthenium complex shows a strong absorption band at 362 nm due to a metal-to-ligand charge transfer transition, $M \rightarrow CO$. In the diffuse reflectance spectrum of the Ru@SH-MWCNT, this band appeared at 355 nm which confirmed the attachment of Ru(CO)₄ to the MWCNT (Fig. 6).

Catalytic activity

In continuation of our interest in developing the catalytic scope of ruthenium as a homogeneous catalyst in the synthesis of xanthenes [21, 44], we decided to investigate the catalytic activity of ruthenium supported on MWCNT as a heterogeneous nano-catalyst for the synthesis of these heterocyclic compounds. Initially, to optimize the reaction condition for the synthesis of 14-aryl-14-*H*-dibenzo[*a,j*]xanthenes, the

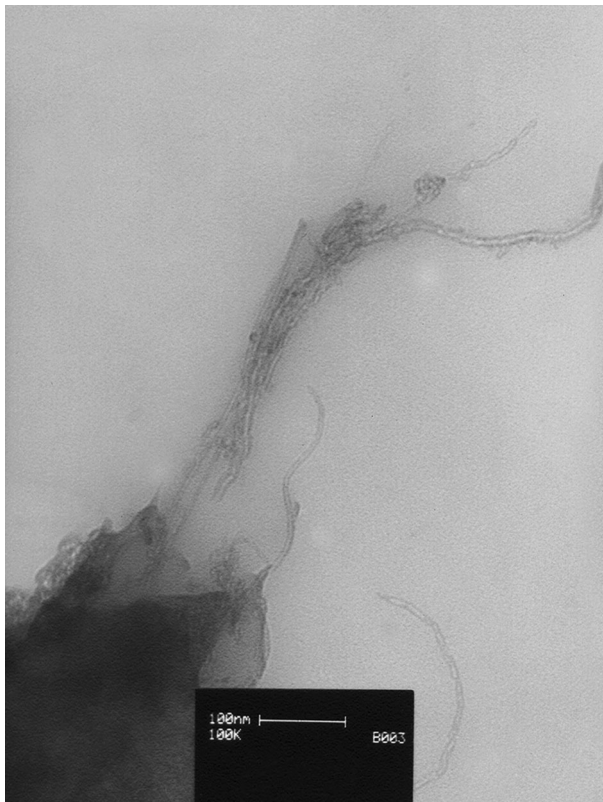


Fig. 4 TEM image of Ru@SH-MWCNT

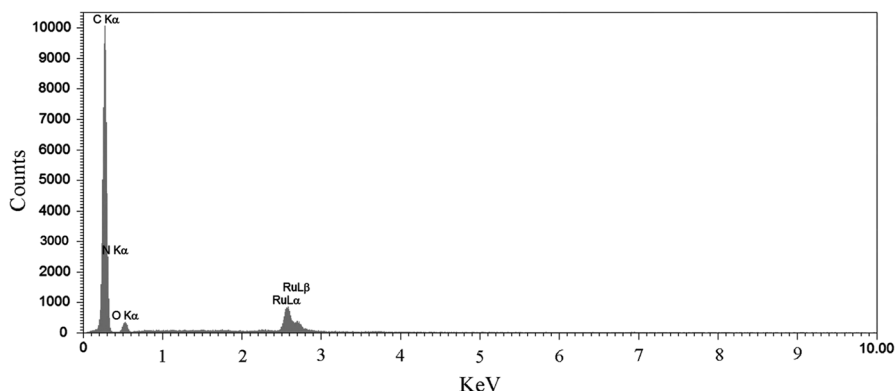


Fig. 5 EDX analysis of Ru@SH-MWCNT

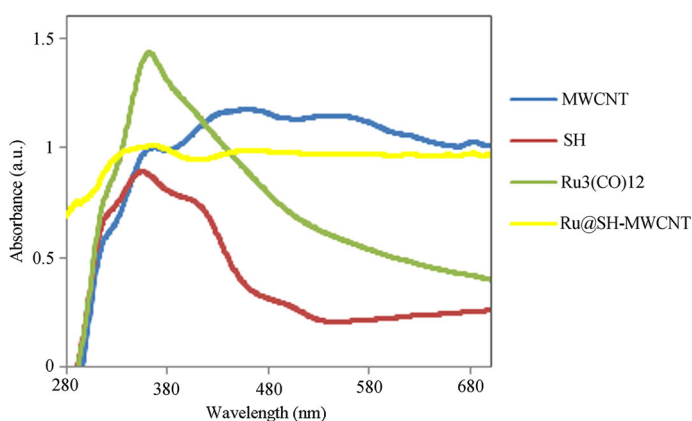


Fig. 6 UV-Vis diffuse reflectance spectra of Ru₃(CO)₁₂, SH, MWCNT and Ru@SH-MWCNT

reaction of β -naphthol (2 mmol) and benzaldehyde (1 mmol) was selected as a model reaction (Scheme 2). The results are shown in Table 2. In order to determine the optimum quantity of catalyst, the reaction was carried out in ethanol at 100 °C in an oil bath in the presence of 5, 10, 15 and 20 wt% of catalyst. The best result was achieved in the presence of 15 wt% of catalyst (Table 2, entry 3). A trace amount of the product was obtained in the absence of catalyst, indicating that the catalyst is necessary for the reaction (Table 2, entry 5). In order to evaluate the role of MWCNT support in the reaction, we carried out the reaction of β -naphthol and benzaldehyde by using 20 wt% of MWCNT as catalyst. The reaction was not completed even after 6 h, and a trace amount of the corresponding xanthenes was formed (Table 2, entry 6). To examine the effect of solvent, the same model reaction in the presence of 15 wt% of the catalyst was performed in the various solvents such as CH₃OH, CH₃CN, CH₂Cl₂ and THF. Ethanol was found to be the best solvent for this reaction. To improve efficiency, we carried out this reaction under ultrasonic irradiation. The best results were obtained by using sonication at 40 °C and 15 wt% of catalyst (Table 2, entry 12).

Table 2 Screening of the reaction condition for the synthesis of 14-phenyl-14-*H*-dibenzo[*a,j*]xanthene (**4a**)

Entry	Solvent	Condition	Cat (wt%)	Time (min)	Yield (%)
1	EtOH	Reflux/100 °C	5	180	70
2	EtOH	Reflux/100 °C	10	150	80
3	EtOH	Reflux/100 °C	15	120	90
4	EtOH	Reflux/100 °C	20	120	90
5	EtOH	Reflux/100 °C	–	360	Trace
6	EtOH	Reflux/100 °C	20	360	Trace ^a
7	MeOH	Reflux/100 °C	15	120	70
8	CH ₃ CN	Reflux/100 °C	15	120	60
9	THF	Reflux/100 °C	15	120	60
10	CH ₂ Cl ₂	Reflux/100 °C	15	120	40
11	EtOH	Ultrasound/30 °C	15	30	88
12	EtOH	Ultrasound/40 °C	15	20	92

^a MWCNT was used as catalyst

Table 3 Synthesis of 14-aryl-14-*H*-dibenzo[*a,j*]xanthenes in the presence of Ru@SH-MWCNT

Entry	Ar	Method A		Method B		M.P. (°C)	
		Time (min)	Yield (%) ^a	Time (min)	Yield (%) ^a	Found	Reported [Ref.]
1	C ₆ H ₅	120	90	20	92	182–184	182–184 [22]
2	4-NO ₂ C ₆ H ₄	60	90	15	94	323–325	324 [13]
3	4-ClC ₆ H ₄	90	92	15	96	301–303	300–302 [18]
4	4-BrC ₆ H ₄	90	94	20	95	297–299	297–298 [11]
5	2-ClC ₆ H ₄	90	88	20	90	216–218	214–216 [11]
6	2,4-Cl ₂ C ₆ H ₃	90	84	20	90	252–254	253–255 [18]
7	4-OHC ₆ H ₄	120	88	25	92	141–143	141–143 [20]
8	4-CH ₃ C ₆ H ₄	150	85	30	88	228–230	229–230 [14]
9	4-CH ₃ OC ₆ H ₄	150	87	30	90	214–216	213–215 [18]
10	3,4-(CH ₃ O) ₂ C ₆ H ₃	180	82	30	90	209–211	208–210 [21]

All products were characterized by ¹H NMR, ¹³C NMR, and IR data

^a Yields refer to the isolated pure products

With the optimized condition in hand, a series of 14-aryl-14-*H*-dibenzo[*a,j*]xanthene derivatives were prepared. The results are listed in Table 3. Various aromatic aldehydes having substituents either electron-releasing or electron-withdrawing groups reacted successfully and resulted in good yields of the corresponding products (Table 3, **4a–4j**). It was found that aromatic aldehydes with electron-withdrawing groups somehow reacted faster than those bearing electron-donating groups. As shown in Table 3, ultrasonics affords the desired products in excellent yields in rather short times.

Table 4 Optimization of the reaction condition for the synthesis of 3,3,6,6-tetramethyl-9-(phenyl)-1,8-dioxooctahydroxanthene (**5a**)

Entry	Solvent	Condition	Cat (wt%)	Time (min)	Yield (%)
1	EtOH	Reflux/80 °C	5	90	65
2	EtOH	Reflux/80 °C	10	60	80
3	EtOH	Reflux/80 °C	15	40	90
4	EtOH	Reflux/80 °C	20	40	90
5	EtOH	Reflux/80 °C	–	360	Trace
6	MeOH	Reflux/65 °C	15	90	75
7	CH ₃ CN	Reflux/80 °C	15	90	60
8	THF	Reflux/70 °C	15	90	50
9	CH ₂ Cl ₂	Reflux/40 °C	15	90	50
10	EtOH	Ultrasound/30 °C	15	20	85
11	EtOH	Ultrasound/40 °C	15	15	92

To further evaluate the efficacy of the catalyst, the condensation reaction of dimedone with aromatic aldehydes for the synthesis of 1,8-dioxo-octahydroxanthene derivatives was studied. In order to optimize the reaction condition, the reaction of benzaldehyde (1 mmol) with dimedone (2 mmol) as a model reaction was carried out under reflux condition and ultrasonic irradiation in the presence of Ru@SH-MWCNT (Scheme 2). The results are given in Table 4, from which it is clear that refluxing in ethanol at 80 °C and sonication at 40 °C in the presence of 15 wt% of catalyst proved to be the optimum condition for this reaction.

For assessing the generality of optimized reaction condition, a wide range of substituted aromatic aldehydes were condensed with dimedone to furnish the corresponding products in high yields (Table 5). The presence of electron-

Table 5 Ru@SH-MWCNT catalyzed synthesis of 1,8-dioxo-octahydroxanthenes

Entry	Ar	Method A		Method B		M.P. (°C)	
		Time (min)	Yield (%) ^a	Time (min)	Yield (%) ^a	Found	Reported [Ref.]
1	C ₆ H ₅	40	90	15	92	202–204	204–205 [30]
2	4-NO ₂ C ₆ H ₄	30	92	10	92	228–230	228–230 [34]
3	4-ClC ₆ H ₄	35	92	15	94	232–234	230–233 [30]
4	4-BrC ₆ H ₄	35	90	15	96	240–242	240–242 [29]
5	4-FC ₆ H ₄	30	94	10	95	227–227	226–227 [32]
6	3-NO ₂ C ₆ H ₃	35	92	20	92	172–174	171–174 [34]
7	2-ClC ₆ H ₄	35	90	20	92	227–229	229–230 [30]
8	2,4-Cl ₂ C ₆ H ₃	40	88	20	90	252–254	253–254 [34]
9	4-CH ₃ OC ₆ H ₄	60	85	30	88	239–241	242–243 [32]
10	3-OHC ₆ H ₃	60	82	35	86	222–224	223–225 [32]

All products were characterized by ¹H NMR, ¹³C NMR, and IR data

^a Yields refer to the isolated pure products

Table 6 Screening of the reaction condition for the synthesis of 9,9-dimethyl-12-phenyl-8,9,10,12-tetrahydrobenzo[*a*]-xanthen-11-one (**6a**)

Entry	Solvent	Condition	Cat (wt%)	Time (min)	Yield (%)
1	EtOH	Reflux/80 °C	5	60	60
2	EtOH	Reflux/80 °C	10	40	70
3	EtOH	Reflux/80 °C	15	30	85
4	EtOH	Reflux/80 °C	20	30	85
5	EtOH	Reflux/80 °C	–	360	Trace
6	MeOH	Reflux/65 °C	15	60	75
7	CH ₃ CN	Reflux/80 °C	15	60	65
8	THF	Reflux/70 °C	15	60	50
9	CH ₂ Cl ₂	Reflux/40 °C	15	60	45
10	EtOH	Ultrasound/30 °C	15	15	85
11	EtOH	Ultrasound/40 °C	15	10	90

Table 7 Synthesis of tetrahydrobenzo[*a*]xanthene-11-ones catalyzed by Ru@SH-MWCNT

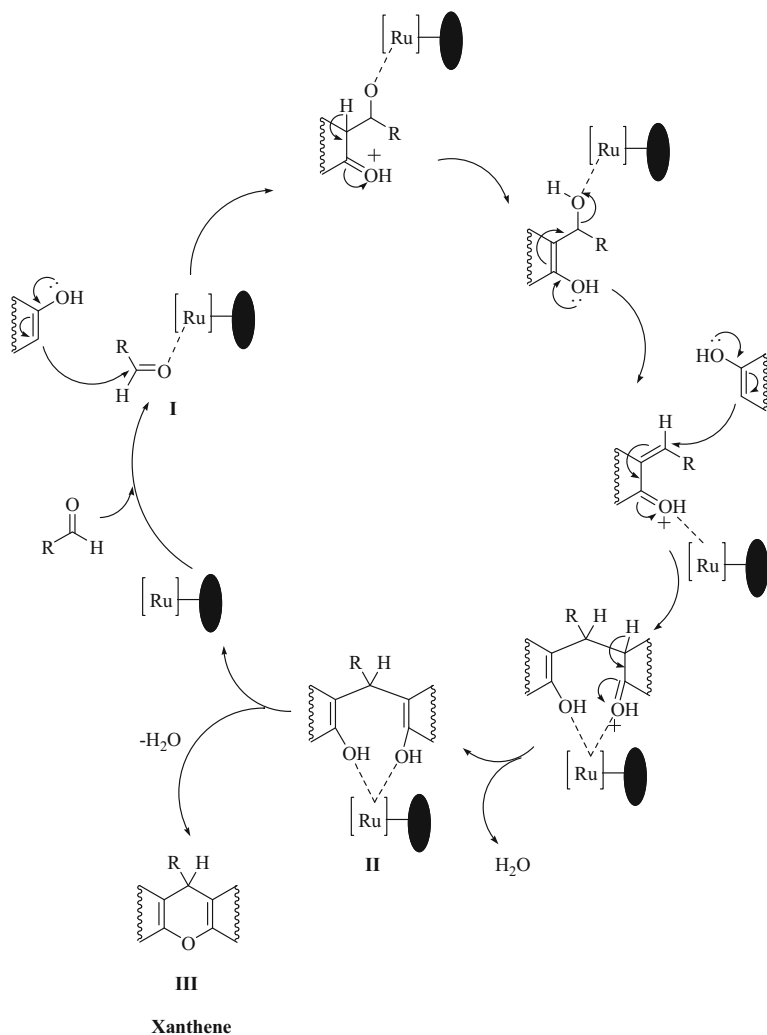
Entry	Ar	Method A		Method B		M.P. (°C)	
		Time (min)	Yield (%) ^a	Time (min)	Yield (%) ^a	Found	Reported [Ref.]
1	C ₆ H ₅	30	85	10	90	150–152	151–153 [38]
2	4-NO ₂ C ₆ H ₄	25	90	10	94	179–181	178–180 [38]
3	4-ClC ₆ H ₄	25	90	10	96	186–188	187–188 [41]
4	3-NO ₂ C ₆ H ₄	35	86	15	90	167–169	167–170 [23]
5	3-ClC ₆ H ₄	30	87	15	92	174–176	175–178 [23]
6	4-CH ₃ OC ₆ H ₄	40	85	20	90	207–209	208–209 [39]
7	3,4-(CH ₃ O) ₂ C ₆ H ₃	45	82	25	88	202–204	201–204 [44]
8	4-SCH ₃ -C ₆ H ₄	45	85	20	90	209–210	209–211 [44]

All products were characterized by ¹H NMR, ¹³C NMR, and IR data

^a Yields refer to the isolated pure products

withdrawing groups on the aromatic ring of aldehydes accelerated the reaction rate. The main advantage of ultrasonic is the significant decrease in the reaction times. As can be seen in Table 5, ultrasonic irradiation affords the respective products in rather short times.

After the successful synthesis of a series of 14-aryl-14-*H*-dibenzo[*a,j*]xanthenes and 1,8-dioxo-octahydroxanthenes, we tried to extend the scope of the present protocol to a three-component reaction for the condensation of aldehydes, β-naphthol and dimedone to afford tetrahydrobenzo[*a*]xanthene-11-one derivatives. Firstly, for the optimization of the reaction condition, the reaction of benzaldehyde (1 mmol), β-naphthol (1 mmol) and dimedone (1.2 mmol) was checked as a model reaction under reflux condition and ultrasonic irradiation. The best results were



Scheme 4 Possible mechanism for the formation of xanthenes in the presence of Ru@SH-MWCNT as catalyst

achieved by carrying out this reaction under refluxing in ethanol and sonication at 40 °C in the present of 15 wt% of catalyst (Table 6).

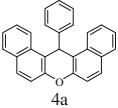
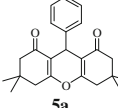
Using these optimized conditions, a variety of aromatic aldehydes were explored to evaluate the substrate scope of this reaction (Table 7). The aromatic aldehydes carrying both electron-withdrawing and electron-donating groups were also converted to the corresponding tetrahydrobenzo[*a*]xanthene-11-one derivatives in good yields (**6a–6h**). These results are presented in Table 7. It was shown that the aromatic aldehydes bearing electron-withdrawing groups reacted faster than those bearing electron-donating groups as would be expected. It can be inferred from

Table 7 that high yields of products were obtained in shorter reaction times under ultrasonic irradiation.

The plausible mechanism for the synthesis of xanthenes in the presence of Ru@SH-MWCNT as a heterogeneous catalyst can be visualized as given in Scheme 4. As shown, prior activation of the carbonyl group of aldehyde by Ru gives intermediate **I**. After two successive nucleophilic attack and loss of water, intermediate **II** undergoes dehydration to afford the desired product (**III**).

A comparison of the catalytic efficiency of Ru@SH-MWCNT to prepare the products of model reactions (**4a** and **5a**) with the results of several other catalytic systems reported in the literature for the same transformations is tabulated in Table 8. As shown, the present protocol is comparable with several of the others.

Table 8 Comparison of our results with those obtained using some of the other catalysts for the synthesis of model compounds **4a** and **5a**

Product	Catalyst (amount)	Reaction conditions	Time (min)	Yield (%)	References
 4a	NH ₄ H ₂ PO ₄ /SiO ₂ (0.1 gr)	US/H ₂ O/40 °C	40	88	[49]
	Mg(HSO ₄) ₂ (0.022 gr)	US/CH ₂ Cl ₂ /reflux	6	95	[51]
	BF ₃ -SiO ₂ (0.08 gr)	US/CHCl ₃ /reflux	6	95	[48]
	Ru@SH-MWCNT (15 wt%)	US/EtOH/40 °C	20	92	This work
 5a	DBSA (10 mol %)	US/H ₂ O/25 °C	60	89	[46]
	[Hbim]BF ₄ (2 mL)	US/CH ₃ OH/30 °C	45	85	[47]
	Ru@SH-MWCNT (15 wt%)	US/EtOH/40 °C	15	92	This work

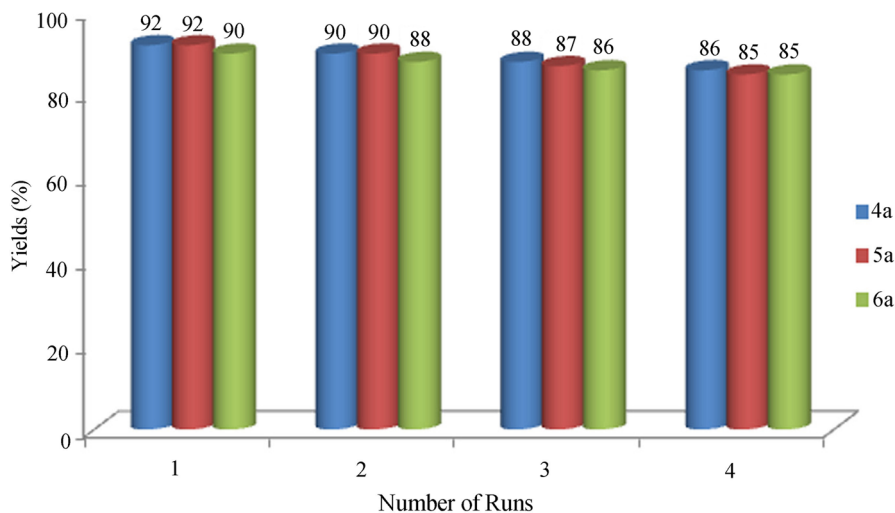


Fig. 7 Reusability of Ru@SH-MWCNT in the synthesis of model compounds **4a**, **5a** and **6a**

Catalyst reusability

Reusability is the principal advantage of a heterogeneous catalyst. The reusability of the catalyst was investigated in the synthesis of model compounds (**4a**, **5a** and **6a**) under ultrasonic irradiation. Upon completion of the reaction, the catalyst was separated, washed thoroughly with ethyl acetate and acetone, dried under vacuum and used again in the same reaction. The catalyst was so efficient that we could use it for four times in succession without significant loss of activity (Fig. 7).

Conclusions

In brief, we have demonstrated that anchorage of ruthenium on MWCNT via functionalization of the support and coordinatively attachment of Ru(CO)₄ results in a novel and effective heterogeneous catalyst for the one-pot synthesis of 14-aryl-14-*H*-dibenzo[*a,j*]xanthene, 1,8-dioxo-octahydroxanthene and tetrahydrobenzo[*a*]xanthene-11-one derivatives (28 samples, up to 96 % yield). Marked improvements offered with this method, such as reusability of the catalyst, high yields of products and low reaction times, make it a useful and attractive strategy for the synthesis of xanthenes.

Acknowledgment The authors are grateful to the Research Council of the University of Guilan for the partial support of this study.

References

1. A. Domling, I. Ugi, *Angew. Chem. Int. Ed.* **39**, 3168 (2000)
2. B.A. Arndtsen, *Chem. Eur. J.* **15**, 302 (2009)
3. J.R. Dimmock, S.K. Raghavan, G.E. Bigam, *Eur. J. Med. Chem.* **23**, 111 (1988)
4. J.J. Omolo, M.M. Johnson, S.F.V. Vuuren, C.B.D. Koning, *Bioorg. Med. Chem. Lett.* **21**, 7085 (2011)
5. G. Saint-Ruf, H.T. Hieu, J.P. Poupelin, *Naturwissenschaften* **62**, 584 (1975)
6. C.G. Knight, T. Stephens, *Biochem. J.* **258**, 683 (1989)
7. M. Ahmad, T.A. King, D.K. Ko, B.H. Cha, J. Lee, *J. Phys. D Appl. Phys.* **35**, 1473 (2002)
8. J.P. Alcantara-Licudine, M.K. Kawate, Q.X. Li, *J. Agric. Food Chem.* **45**, 766 (1997)
9. B. Rajitha, B.S. Kumar, Y.T. Reddy, P.N. Reddy, N. Sreenivasulu, *Tetrahedron Lett.* **46**, 8691 (2005)
10. M.A. Pasha, V.P. Jayashankara, *Bioorg. Med. Chem. Lett.* **17**, 621 (2007)
11. M.A. Bigdeli, M.M. Heravi, G.H. Mahdavinia, *Catal. Commun.* **8**, 1595 (2007)
12. M.A. Bigdeli, M.M. Heravi, G.H. Mahdavinia, *J. Mol. Catal. A Chem.* **275**, 25 (2007)
13. M.M. Heravi, K. Bakhtiari, Z. Daroogheha, F.F. Bamoharram, *J. Mol. Catal. A Chem.* **273**, 99 (2007)
14. A.K. Bhattacharya, K.C. Rana, *Mendeleev Commun.* **17**, 247 (2007)
15. G. Imani Shakibaei, P. Mirzaei, A. Bazgir, *Appl. Catal. A Gen.* **325**, 188 (2007)
16. W. Su, D. Yang, C. Jin, B. Zhang, *Tetrahedron Lett.* **49**, 3391 (2008)
17. M. Dabiri, M. Baghbanzadeh, M.S. Nikcheh, E. Arzroomchilar, *Bioorg. Med. Chem. Lett.* **18**, 436 (2008)
18. S. Kantevvari, M.V. Chary, P.R. Das, S.V.N. Vuppalapati, N. Lingaiah, *Catal. Commun.* **9**, 1575 (2008)
19. J. Li, L. Lu, W. Su, *Tetrahedron Lett.* **51**, 2434 (2010)
20. A. Zarei, A.R. Hajipour, L. Khazdooz, *Dyes Pigments* **85**, 133 (2010)

21. K. Tabatabaieian, A. Khorshidi, M. Mamaghani, A. Dadashi, *Synth. Commun.* **41**, 1427 (2011)
22. G.B.D. Rao, M.P. Kaushik, A.K. Halve, *Tetrahedron Lett.* **53**, 2741 (2012)
23. M.A. Zolfigol, V. Khakyzadeh, A.R. Moosavi-Zare, A. Zare, S.B. Azimi, Z. Asgari, A. Hasaninejad, *C. R. Chim.* **15**, 719 (2012)
24. M. Mokhtary, S. Refahati, *Dyes Pigments* **99**, 378 (2013)
25. H. Naeimi, Z.S. Nazifi, *Appl. Catal. A Gen.* **477**, 132 (2014)
26. F. Shirini, A. Yahyazadeh, K. Mohammadi, *Chin. Chem. Lett.* **25**, 341 (2014)
27. T.S. Jin, J.S. Zhang, J.C. Xiao, A.Q. Wang, T.S. Li, *Synlett* **5**, 866 (2004)
28. B. Das, P. Thirupathi, I. Mahender, V.S. Reddy, Y.K. Rao, *J. Mol. Catal. A Chem.* **247**, 233 (2006)
29. S. Kantevari, R. Bantu, L. Nagarapu, *ARKIVOC* **xvi**, 136 (2006)
30. G. Song, B. Wang, H. Luo, L. Yang, *Catal. Commun.* **8**, 673 (2007)
31. F. Darviche, S. Balalaie, F. Chadegani, P. Salehi, *Synth. Commun.* **37**, 1059 (2007)
32. Z.H. Zhang, Y.H. Liu, *Catal. Commun.* **9**, 1715 (2008)
33. M. Seyyedhamzeh, P. Mirzaei, A. Bazgir, *Dyes Pigments* **76**, 836 (2008)
34. H.R. Shaterian, A. Hosseinian, M. Ghashang, *Turk. J. Chem.* **33**, 233 (2009)
35. A. Zare, A.R. Moosavi-Zare, M. Merajoddin, M.A. Zolfigol, T. Hekmat-Zadeh, A. Hasaninejad, A. Khazaei, M. Mokhlesi, V. Khakyzadeh, F. Derakhshan-Panah, M.H. Beyzavi, E. Rostami, A. Arghoon, R. Roohandeh, *J. Mol. Liq.* **167**, 69 (2012)
36. J. Li, W. Tang, L. Lu, W. Su, *Tetrahedron Lett.* **49**, 7117 (2008)
37. J.M. Khurana, D. Magoo, *Tetrahedron Lett.* **50**, 4777 (2009)
38. G.C. Nandi, S. Samai, R. Kumar, M.S. Singh, *Tetrahedron* **65**, 7129 (2009)
39. R.Z. Wang, L.F. Zhang, Z.S. Cui, *Synth. Commun.* **39**, 2101 (2009)
40. S. Gao, C.H. Tsai, C.F. Yao, *Synlett* **2009**, 949 (2009)
41. Z.H. Zhang, H.J. Wang, X.Q. Ren, Y.Y. Zhang, *Monatsh. Chem.* **140**, 1481 (2009)
42. H.J. Wang, X.Q. Ren, Y.Y. Zhang, Z.H. Zhang, *J. Braz. Chem. Soc.* **20**, 1939 (2009)
43. A. Kumar, S. Sharma, R.A. Maurya, J. Sarkar, *J. Comb. Chem.* **12**, 20 (2010)
44. K. Tabatabaieian, A. Khorshidi, M. Mamaghani, A. Dadashi, M.K. Jalali, *Can. J. Chem.* **89**, 623 (2011)
45. F. Shirini, N.G. Khaligh, *Dyes Pigments* **95**, 789 (2012)
46. T.S. Jin, J.S. Zhang, A.Q. Wang, T.S. Li, *Ultrason. Sonochem.* **13**, 220 (2006)
47. K. Venkatesan, S.S. Pujari, R.J. Lahoti, K.V. Srinivasan, *Ultrason. Sonochem.* **15**, 548 (2008)
48. B.B.F. Mirjalili, A. Bamoniri, A. Akbari, *Tetrahedron Lett.* **49**, 6454 (2008)
49. G.H. Mahdavinia, S. Rostamizadeh, A.M. Amani, Z. Emdadi, *Ultrason. Sonochem.* **16**, 7 (2009)
50. S. Rostamizadeh, A.M. Amani, G.H. Mahdavinia, G. Amiri, H. Sepehrian, *Ultrason. Sonochem.* **17**, 306 (2010)
51. B.B.F. Mirjalili, A. Bamoniri, A. Akbari, *Chin. Chem. Lett.* **22**, 45 (2011)
52. N.G. Khaligh, *Ultrason. Sonochem.* **19**, 736 (2012)
53. S.I. Murahashi, *Ruthenium in Organic Synthesis* (Wiley, New York, 2004)
54. C. Bruneau, P.H. Dixneuf, *Ruthenium Catalysts and Fine Chemistry* (Springer, Berlin, 2004)
55. T. Naota, H. Takaya, S.I. Murahashi, *Chem. Rev.* **98**, 2599 (1998)
56. J.W. Kim, K. Yamaguchi, N. Mizuno, *J. Catal.* **263**, 205 (2009)
57. S.M. Islam, K. Tuhina, M. Mubarak, P. Mondal, *J. Mol. Catal. A Chem.* **297**, 18 (2009)
58. P. Veerakumar, Z.Z. Lu, M. Velayudham, K.L. Lu, S. Rajagopal, *J. Mol. Catal. A Chem.* **332**, 128 (2010)
59. M. Hatefi, M. Moghadam, V. Mirkhani, I. Sheikhshoei, *Polyhedron* **29**, 2953 (2010)
60. C.H. Yen, H.W. Lin, C.S. Tan, *Catal. Today* **174**, 121 (2011)
61. D. Tasis, N. Tagmatarchis, A. Bianco, M. Prato, *Chem. Rev.* **106**, 1105 (2006)
62. J.N. Coleman, U. Khan, W.J. Balu, Y.K. Gunko, *Carbon* **44**, 1624 (2006)
63. M. Moghadam, I. Mohammadpoor Baltork, S. Tangestaninejad, V. Mirkhani, H. Kargar, N. Zeini-Isfahani, *Polyhedron* **28**, 3816 (2009)
64. M. Moghadam, S. Tangestaninejad, V. Mirkhani, I. Mohammadpoor Baltork, N.S. Mirbagheri, *J. Organomet. Chem.* **695**, 2014 (2010)
65. S. Tangestaninejad, M. Moghadam, V. Mirkhani, I. Mohammadpoor Baltork, M.S. Saeedi, *Appl. Catal. A Gen.* **381**, 233 (2010)
66. B. Barati, M. Moghadam, A. Rahmati, V. Mirkhani, S. Tangestaninejad, I. Mohammadpoor Baltork, *J. Organomet. Chem.* **724**, 32 (2013)
67. K. Tabatabaieian, M.A. Zanjanchi, M. Mamaghani, A. Dadashi, *Can. J. Chem.* **92**, 1086 (2014)
68. C. Sousa, C. Freire, B.D. Castro, *Molecules* **8**, 894 (2003)

69. Y. Liu, L. Gao, *Carbon* **43**, 47 (2005)
70. A. Tarlani, K. Narimani, F. Mohammadipanah, J. Hamed, H. Tahermansouri, M.M. Amini, *Appl. Surf. Sci.* **341**, 86 (2015)
71. F. Gao, J. Li, F. Kang, Y. Zhang, X. Wang, F. Ye, J. Yang, *J. Phys. Chem. C* **115**, 11822 (2011)